CoA Note No. 41

THE COLLEGE OF AERONAUTICS

CRANFIELD

THE EFFECT OF TRANSITION WIRES ON THE PRESSURE DISTRIBUTION OVER A N.A.C.A. 63A215 AEROFOIL SECTION

by

K. D. HARRIS

TECHNICAL NOTE No. 41
FEBRUARY, 1956.

THE COLLEGE OF AERONAUTICS

CRANFIELD

The effect of transition wires on the pressure distribution over a N.A.C.A. 63A215 aerofoil section.

-by-

K. D. Harris, B.Sc. (Eng.), D.C.Ae., A.F.R.Ae.S.

SUMMARY

Pressure distributions have been measured over the surface of a N.A.C.A. 63A215 aerofoil section to determine the effect of transition wires on the lift and pitching moment characteristics. These tests, which were made at Reynolds numbers of 3×10^5 and 8×10^5, showed that with transition left free laminar separation, followed by turbulent re-attachment, occurred at about 60% chord at low incidences. At medium incidence the position of laminar separation and turbulent re-attachment moved rapidly forward giving rise to kinks or non-linearities in the lift curve.

The addition of transition wires at 27½% chord eliminated the laminar separation at low incidences and thereby caused the lift curve to become more nearly linear. However, the wires resulted in a reduction in the lift-curve slope at the design C_L, and a reduction in $C_{L_{max}}$.

Transition wires at 8%, 4% or 1% chord were found to have very adverse effects on the aerofoil characteristics. In particular the lift curves were made very non-linear, and $C_{L_{max}}$ was reduced. The non-linearity was caused by sudden changes in the boundary layer with change of incidence.

PDF

CONTENTS

Diagrams and Figures

1. Diagram of model
2. Lift characteristics
3. Pitching moment characteristics ($R = 3 \times 10^5$)
4. Pitching moment characteristics ($R \triangleq 8 \times 10^5$)
5. Upper surface pressure distributions
   (a) $\alpha_G = -2^\circ$
   (b) $\alpha_G = 6^\circ$
   (c) $\alpha_G = 10^\circ$
   (d) $\alpha_G = 14^\circ$
6. Comparison of pressure distributions near the stall at two values of the Reynolds number.
7. The approximate chordwise positions of laminar separation, turbulent re-attachment and turbulent separation.
8. Comparison of lift-curve slopes for test section (N.A.C.A. 63A215) with N.A.C.A. section 64A212.

1. Notation

c = chord

C_c = chordwise force coefficient

C_L = lift coefficient

C'_L = lift coefficient uncorrected for tunnel interference

$C_{m_{\frac{1}{4}}}$ = pitching moment coefficient measured about the quarter chord point

$C'_{m_{\frac{1}{4}}}$ = pitching moment coefficient uncorrected for tunnel interference

C_N = normal force coefficient

C_p = pressure coefficient
$= (p-p_A)/\frac{1}{2}\rho V^2$

h = effective height of working section

h_o = distance of the aerodynamic centre aft of the leading edge measured as a fraction of the chord c.

p = static pressure on aerofoil surface

p_A = atmospheric pressure

p_c = static pressure at entry to wind tunnel contraction

q = dynamic pressure
$= \frac{1}{2}\rho V^2$

R = Reynolds number based on chord c
$= \frac{\rho V c}{\mu}$

V = wind speed.

Axes xy are taken with origin at the leading edge, the x-axis being coincident with the chord line and the y-axis being perpendicular to the x-axis.

α = wing incidence (corrected for tunnel interference)

α_G = geometric wing incidence

μ = coefficient of viscosity of the air

ρ = density of the air

2. Introduction

The tests described in this report were undertaken as a result of a request that the College should make a series of stability and control tests on a wind tunnel model of an aeroplane having a wing of aspect ratio 20. Since the largest tunnel available for these tests was one with a working section $3\frac{1}{2}$ feet in diameter, and a top speed of about 140 feet per second, it followed that the Reynolds number of the tip section of the model wing would only be about 1×10^5. Concern was felt lest the results obtained at such a low Reynolds number might differ appreciably from the flight characteristics at the full scale Reynolds number of about 2×10^6. It was therefore decided to investigate the characteristics of the tip section over the widest possible range of Reynolds number available in the wind tunnel to see if by the use of transition wires the characteristics at $R = 1 \times 10^5$ could be made similar to the characteristics at $R = 2 \times 10^6$. To obtain sufficiently detailed information it was decided to pressure plot a relatively large model of the tip section. The results obtained are of considerable interest, and because of the dearth of published information on pressure distributions with and without transition wires it was felt that some use might be served by publishing the present results. It should be pointed out however that the tunnel interference corrections which had to be applied were large and somewhat approximate owing to the fact that no published correction data is available for the particular configuration of model and tunnel that was used.

3. Description of Apparatus

The model, which is illustrated in Figure (1), consisted of a rectangular wing of chord 1 foot and span 3 feet, with oval shaped endplates attached to the tips. The aerofoil section was N.A.C.A. 63A215, the ordinates of which are given in Table I.

Spanwise pressure tubes were let into the upper and lower surfaces of the model at the following chordwise positions :-

$\frac{x}{c}$ = 0, 0.025, 0.05, 0.075, 0.10, and thereafter at intervals of 0.05 back to x/c = 0.80.

The model was constructed of wood, and, as originally supplied, the aerofoil section was far from accurate. The model was therefore improved by modifying the section over the mid portion of the span where the pressure holes were situated.

The tests were made in the College of Aeronautics 'No.2 Wind Tunnel'. This tunnel has a circular-section, open-jet working section of diameter $3\frac{1}{2}$ feet, and a top speed of about 140 feet per second.

The incidence of the model relative to the horizontal was measured by means of a sensitive inclinometer, and the pressure distributions were measured on a tilting multi-tube manometer containing methylated spirits.

4. Details of Test

Pressure distribution measurements were made at two wind speeds. These speeds were chosen to give the greatest practicable range of Reynolds number. The lower speed, which was determined by considerations of the accuracy of the observed results, was 46.8 feet per second. The upper speed, which was chosen as the maximum available tunnel speed, varied from about 132 feet per second at low incidence to about 115 feet per second at the maximum test incidence. The low speed tests gave a Reynolds number of 3×10^5 based on the wing chord of 1 foot, whereas the high speed tests gave a mean Reynolds number of about 8×10^5.

To obtain a high degree of repeatability in setting the incidence an inclinometer was used in preference to the incidence telescope. Use of the inclinometer necessitated stopping the tunnel each time the incidence was changed. This may have influenced the results obtained at the higher incidences, but this was not considered important because the stalling behaviour of the aerofoil was not the object of investigation.

Tests were made with transition free and with transition wires attached to both the upper and lower surfaces at $27\frac{1}{2}\%$, 8%, 4% and 1% of the chord aft of the leading edge.

The diameter of the wire used was 0.028" ; attachment to the wing surface was by means of chordwise strips of adhesive tape.

The pressure distributions were measured on a tilting multi-tube manometer. The static pressure in the working section was assumed to be exactly atmospheric. The dynamic pressure was measured by a static tapping taken from the entry to the contraction. Calibration of the empty tunnel shows that the dynamic pressure q ($= \frac{1}{2}\rho V^2$) is given by the formula :-

$$q = (p_c - p_A).$$

However, as described in the Appendix, it was found that with the model in the tunnel the tunnel calibration factor was not a constant, and the following approximate formula was deduced :-

$$q = (1 + 0.05\ C_L')(p_c - p_A).$$

5. Presentation of results

5.1 C_p distributions

The C_p distributions are given in Tables III and IV. A few selected distributions are plotted in Figures (5) and (6). It should be noted that no corrections for tunnel interference effects have been applied to either the tabulated or plotted distributions.

5.2 Lift and pitching moment results

The lift and pitching moment coefficients are given in Table II. In Figure (2) C_L is plotted against α, and in Figures (3) and (4) $C_{m_{1/4}}$ is plotted against C_L. These results have all been fully corrected by the methods outlined in the Appendix.

For the reasons given in the Appendix no drag results are given.

5.3 Lift-curve slope and aerodynamic centre

In most of the test configurations the $C_L \sim \alpha$ curves were not linear. The lift-curve slopes quoted below have therefore been evaluated at the section design C_L of 0.2. The aerodynamic centre positions have likewise been evaluated at a C_L of 0.2. In certain cases reliable values of lift-curve slope and aerodynamic centre are not obtainable from the measured results. Where this is the case a question mark (?) has been placed in the appropriate space.

Distance of transition wire aft of leading edge (x/c)	$dC_L/d\alpha$ R ÷ 10^5		h_o R ÷ 10^5	
	3	8	3	8
No wires	5.4	5.4	0.245	0.245
0.275	5.0	5.1	0.225	0.230
0.08	5.0	5.0	0.225	0.240
0.04	4.4	?	0.220	0.230
0.01	5.0	4.7(5)	0.250	?

The lift-curve slopes have been quoted to the nearest 0.1, and the aerodynamic centre positions to the nearest 0.005. It is considered that whilst the absolute values may not be accurate to within these limits (on account of the uncertain tunnel interference corrections and the lack of sufficient pressure holes) the quoted values are repeatable to within these limits.

6. Discussion

6.1 Lift characteristics (Figure 2)

The fully corrected lift results are plotted in Figure (2), where, to facilitate comparison of the results, the linear lift curve obtained at R = 3 x 10^5 with transition wires at 27½% of the chord has been plotted against each set of results*.

*This reference curve extends beyond the incidence range for which the lift curve at R = 3 x 10^5 is linear.

Generally speaking it will be seen that the lift curves are appreciably more linear with the transition wires at 27½% chord than with no transition wires. However, wires at 8%, 4% or 1% chord make the lift characteristics progressively less linear. These features are all more marked at the lower Reynolds number of 3×10^5.

From the Table in Section 5 it will be seen that the addition of the transition wires results in a reduction in the lift-curve slope at the design C_L. In general the reduction in lift-curve slope increases as the wires are moved towards the leading edge. An exception to this behaviour occurs at the lower Reynolds number when the transition wire is brought right forward to 1% chord. This is due to the fact that the wire is then in a strongly favourable pressure gradient, and the Reynolds number of the boundary layer (based on its thickness) is small. As a result of this the wire causes some thickening of the laminar boundary layer but does not cause transition to turbulent flow.

The kinks and non-linearities in the lift curves are caused by changes in the boundary layers with change of incidence. These changes are discussed in subsections 3, 4 and 5 of the present Section.

6.2 Pitching moment characteristics (Figures 3 and 4)

The $C_m \sim C_L$ curves plotted in Figures 3 and 4 are moderately linear except at incidences where the lift curves become markedly non-linear. The results tabulated in Section 5 show that at the design C_L the aerodynamic centre of the section is at 24.5% of the chord with transition free. The addition of transition wires at 27½% chord moves the aerodynamic centre forward. This is due to the thickening of the boundary layer aft of the wires. As the wires are moved forward towards the leading edge the tendency is for the aerodynamic centre to move slightly further forward. The opposite effect occurs at the lower Reynolds number when the wire is moved forward to the foremost position of 1% chord. This is due to the fact that at low incidences the wire does not cause transition to turbulence and so does not cause any appreciable thickening of the boundary layer.

6.3 The effect of transition wires on the upper surface pressure distributions. (Figures 5a to 5d)

The pressure distributions plotted in Figures 5a to 5d are confined to the upper surface and to a Reynolds number of 3×10^5. This is because the main points of interest are confined to the upper surface, and because the results at the higher Reynolds number are very similar to those at the lower value.

Figure 5a ($\alpha_G = -2^\circ$)

Referring first to the pressure distributions at $\alpha_G = -2^\circ$ it will be seen that with no transition wires there is a short region of approximately constant pressure at about 60% of the chord and that this is followed by a fairly rapid rise in pressure. This feature is eliminated with transition wires at 27½% and with wires at 8% chord, but it re-appears when the wires are moved forward to 4% or 1% chord.

The explanation of this phenomenon is well known. The region of approximately constant pressure coincides with a region of laminar separation, whilst the region of rapid pressure recovery coincides with a region in which the boundary layer changes from laminar to turbulent and re-attaches to the surface as a turbulent layer. In this region the boundary layer displacement thickness decreases rapidly, and it is this which causes the rapid increase of static pressure. Laminar separations of this type have been studied experimentally by Bursnall and Loftin(2) ; and Owen and Klanfer(3) have shown that this type of bubble falls into the category termed 'short bubbles'.

Figure 5b ($\alpha_G = 6^\circ$)

At $\alpha_G = 6^\circ$ the region of laminar separation is still at about the same chordwise position as at $\alpha_G = -2^\circ$, but it appears that transition to turbulence and re-attachment takes place more rapidly after the onset of separation. The addition of the transition wires evidently causes transition to turbulent flow close to the wire irrespective of the location of the wire.

Figure 5c ($\alpha_G = 10^\circ$)

At $\alpha_G = 10^\circ$ the region of natural transition to turbulent flow has moved forward close to the leading edge. With no transition wires it appears that there is probably a short region of laminar separation at about 5% chord followed by almost immediate transition and re-attachment.

Whilst the form of the pressure distribution curves (except in the immediate vicinity of the wires) is very similar for all positions of the transition wires it can be seen that over the forward 40% of the chord there is a distinct reduction of the suction with the wires attached to the aerofoil, and this tends to increase as the wire is moved towards the leading edge. The explanation of this is that the wire causes the turbulent boundary layer downstream of the wire to be thickened. Reference to Figure 5c will show that the reduced suctions over the forward part of the upper surface give rise to reduced values of the lift coefficient.

Figure 5d ($\alpha_G = 14^\circ$)

At $\alpha_G = 14^\circ$ the boundary layer is turbulent from near the leading edge irrespective of the position of the transition wire. It is evident though that as the wire is moved towards the leading edge there is a gradual increase in the extent of the separated flow near the trailing edge. At both values of the Reynolds number and for all positions of the transition wire the stall is caused by a turbulent separation starting at the trailing edge. The effect of the addition of a transition wire is therefore to decrease the stalling value of the lift coefficient. This is clearly shown in Figure 2 where it will be seen that $C_{L_{max}}$ falls progressively as the transition wire is moved towards the leading edge.

6.4 The effect of Reynolds number on the pressure distribution near the stall.

Figure 6 compares the pressure distributions measured at $\alpha_G = 18^\circ$ at Reynolds numbers of 3×10^5 and 7.4×10^5, with transition free.

The first point to be noted is that the boundary

layer separates on the upper surface at about 60% of the chord for both values of the Reynolds number.

The other feature of interest is that whilst over the whole of the lower surface and over much of the upper surface the pressure distributions are almost identical there is a region from the leading edge back to about 10% chord on the upper surface where the distributions differ quite markedly. This is probably associated with differences in the transition of the boundary layer from laminar to turbulent. At the lower Reynolds number there is fairly certain evidence that there is a region of laminar separation at about 4% chord followed by turbulent re-attachment at about 6% chord. At the higher Reynolds number there may be a somewhat similar behaviour, but if this is so the transition to turbulence probably takes place very shortly aft of the position of separation*.

6.5 The approximate chordwise positions of laminar separation, turbulent re-attachment and turbulent separation on the upper surface.

In Figure 7 an attempt has been made to indicate the approximate chordwise positions of laminar separation, turbulent re-attachment and turbulent separation on the upper surface over the full C_L range. These curves are for transition free. This plot is necessarily approximate as the positions at which these flow changes take place have had to be deduced from the pressure distributions. The curves are particularly approximate in the range where the position of transition is varying rapidly with change of lift coefficient. Indeed, although tentative curves have been plotted indicating the positions

*This statement is based on theoretical reasoning rather than on the measured pressure distribution curves. Theory (see Ref.5, p.124) predicts that the position of laminar separation is independent of Reynolds number (provided the pressure distribution up to the point of separation is itself independent of Reynolds number). It is furthermore a well known fact that the position of transition from laminar to turbulent flow in the boundary layer moves towards the front stagnation point as the Reynolds number increases.

of laminar separation and turbulent re-attachment the experimental results are not sufficient to assert that separation definitely takes place in this regime.

It is interesting to note that the regimes where rapid changes of the boundary layer occur correspond with the regimes where the lift curves of Figure 2 are kinked or distinctly non-linear.

6.6 A comparison of the lift-curve slopes of the test section (N.A.C.A. 63A215) and N.A.C.A. section 64A212.

In Figure 8 the lift-curve slopes obtained from the present series of tests are compared with measurements made by the N.A.C.A. (4) on a slightly different section (N.A.C.A. 64A212). The latter measurements, which were made over a Reynolds number range varying from 7×10^5 to 9×10^6, enable some useful deductions to be drawn. In the first place it will be seen that at $R = 8 \times 10^5$ the results of the present experiment agree quite closely with the N.A.C.A. results. Because of the similarity of the two aerofoil sections it would appear reasonable to assume that the variation of lift-curve slope with Reynolds number will be the same for the two sections. Assuming this to be the case we see that at $R = 2 \times 10^6$, which corresponds approximately to the full scale Reynolds number of the tip section of the project, the lift curve slope is about 5.5(5). From the present tests at $R = 3 \times 10^5$ the lift-curve slope is 5.4 with transition free and 5.0 with transition wires at 27½% chord. This suggests that the low incidence characteristics of the complete aircraft will best be simulated by a wind tunnel model having free transition on the wings. On the other hand, for tests at medium to high incidence it might be desirable to use a transition wire at about 30% chord to eliminate the kinks in the lift curve which are associated with the rapid forward movement of the transition point.

The results of the test show that for Reynolds numbers less than 0.8×10^6 laminar separation does not occur until aft of 50% chord in the low incidence range. Thus, if for any reason it was deemed advisable to use transition wires for low incidence tests it might be best to place the wires as far aft as 50% chord. This

would probably lead to a slightly smaller loss in the lift-curve slope due to the addition of the wires. In addition some slight reduction in the loss of lift-curve slope might be achieved by the use of a smaller diameter wire.

7. Conclusions

From the foregoing discussion it is concluded that for low incidence tests on complete models having a N.A.C.A. 63A215 section the best results will be obtained with transition left free on the wings. However, to avoid kinks in the lift and pitching moment curves it may be desirable to use transition wires on the wings for tests at medium to high incidence. The present tests show that such wires should be placed at least as far back as 30% of the chord. It is also tentatively suggested that if transition wires are used for low incidence tests some slight benefit might accrue from placing these wires as far aft as 50% chord.

At low values of incidence laminar separation occurs on the plain wing at about 60% of the chord on the upper surface and this is followed by turbulent re-attachment a little further downstream. At moderate incidence the region of transition from laminar to turbulent flow moves rapidly forward towards the leading edge. This rapid movement is associated with kinks or non-linearities in the lift curves.

At high values of incidence there appears to be a short separation bubble on the upper surface near the leading edge. The available measurements are however not sufficiently detailed for any firm conclusions to be drawn regarding the nature of the boundary layer at slightly lower incidences except to say, as stated previously, that the position of transition moves rapidly forwards with increase of incidence in this incidence range.

The stall occurs through the gradual growth of a turbulent separation which starts at the trailing edge at a C_L of about 0.9 and spreads forward with increase of incidence.

Transition wires at 27½% chord eliminate the laminar separation at low incidences and thereby cause the $C_L \sim \alpha$ curves to become more linear. However, the wires result in a reduction in the lift-curve slope at low incidence and a reduction in $C_{L_{max}}$.

Transition wires near the leading edge generally have a very adverse effect on the aerofoil characteristics. At low incidences they do not necessarily cause transition to turbulence, whilst at medium incidences they cause the point of transition to move suddenly forward giving rise to kinks in the $C_L \sim \alpha$ curves. Also, by thickening the boundary layer at high incidence, they cause a reduction in the $C_{L_{max}}$ of the section.

8. Acknowledgements

Acknowledgement is due to Mr. and Mrs. Hanning-Lee who prompted this work and supplied the model. The author would also like to thank Mr. G. G. Appleby and Mr. P. E. W. Sharman who helped to conduct the experimental work.

9. References

1. Pankhurst, R.C. and Holder, D.W.
Wind Tunnel Technique.
Pitman.

2. Bursnall, W.J. and Loftin, K.L.
Experimental investigation of localised regions of laminar boundary layer separation.
N.A.C.A. T.N. 2338.

3. Owen, P. R. and Klanfer, L.
On the laminar boundary layer separation from the leading edge of a thin aerofoil.
R.A.E. Report No. Aero.2508.

4. Loftin, K.L. and Smith, H.A.

Aerodynamic characteristics of 15 N.A.C.A. airfoil sections at seven Reynolds numbers from 0.7 x 10^6 to 9.0 x 10^6.

N.A.C.A. T.N. 1945

5. Goldstein, S. (Editor)

Modern Developments in Fluid Dynamics (Vol. I)

Oxford University Press.

APPENDIX

Evaluation of uncorrected lift and pitching moment coefficients.

The non-dimensional pressure distributions were plotted against x/c and y/c and integrated by means of an integrator to find the coefficients C_N, C_c and $C'_{m_{1/4}}$. The uncorrected lift coefficient C'_L was then calculated by means of the formula

$$C'_L = C_N \cos \alpha_G - C_c \sin \alpha_G.$$

Owing to the relatively few pressure holes near the leading edge and to the lack of pressure holes over the rear 20% of the chord the chordwise force coefficient C_c could be determined only very approximately. For this reason no attempt was made to evaluate the drag of the aerofoil. (In any case the drag obtained would have been purely the form drag since no measurements of the skin friction or overall drag were made.)

Blockage correction

From Reference 1 pp. 334 and 335 the blockage correction at zero lift is found to be approximately $\frac{1}{4}\%$ on the velocity. Since this is well within the limits of experimental accuracy this correction has been neglected. No published information is available regarding the blockage at other than zero lift, but it was observed that the maximum obtainable tunnel speed

fell appreciably as the incidence was increased. At the same time it was observed that the apparent stagnation pressure coefficient rose from 1.00 at $\alpha_G = 0^o$ to about 1.05 at $\alpha_G = 16^o$. This indicated that the tunnel calibration factor, which was known to be 1.00 for the working section empty, must have risen from 1.00 at low C_L' to about 1.05 at a C_L' of about 1.0. Evidence of the variation of the tunnel calibration factor at intermediate values of C_L' was not obtained and it was therefore assumed that the factor would vary linearly with C_L'. Accordingly the dynamic pressure q was assumed to be given by the formula

$$q = (1 + 0.05\ C_L')(p_c - p_A).$$

Lift and pitching moment corrections for tunnel interference effects.

The corrections to be applied to the observed lift and pitching moment results for tunnel interference effects are necessarily approximate owing to the fact that :-

(i) the tests were made in a circular-section, open-jet tunnel, and

(ii) the model was fitted with finite area end-plates.

Tunnel interference corrections have not been computed for the above case. The nearest case for which corrections have been published is the case of two-dimensional tests* in a rectangular-section, open-jet tunnel. In the absence of any better information it has been assumed that the corrections to be applied to the mid span station of the model in this test are the same as the corrections to be applied to the case for the rectangular-section, open-jet tunnel, except that the effective height (h) of the circular section tunnel is to be taken as the mean height over the span of the model, i.e. h = 3.1 feet.

---

*This implies infinite area end-plates.

With the above approximation the tunnel interference corrections as given in Reference 1 are (in the present notation) :-

$$\left.\begin{aligned} C_L &= C'_L + \frac{\pi^2}{24}\left(\frac{c}{h}\right)^2 C'_L \\ \alpha &= \alpha_G - \frac{\pi}{48}\left(\frac{c}{h}\right)^2\left(C'_L + 4C'_{m_{1/4}}\right) - \frac{1}{4}\left(\frac{c}{h}\right)C'_L \\ C_{m_{1/4}} &= C'_{m_{1/4}} - \frac{\pi^2}{96}\left(\frac{c}{h}\right)^2 C'_L \end{aligned}\right\}$$

Substituting for c and h these formulae become :-

$$\left.\begin{aligned} C_L &= 1.0427\ C'_L \\ \alpha &= \alpha_G - 0.0873\ C'_L - 0.0272\ C'_{m_{1/4}} \\ C_{m_{1/4}} &= C'_{m_{1/4}} - 0.0103\ C'_L \end{aligned}\right\}$$

where α and α_G are measured in radians.

Ordinates of N.A.C.A. 63A215

x/c	y_u/c	$-y_\ell/c$
0	0	0
0.025	0.028	0.023
0.050	0.040	0.032
0.075	0.049	0.038
0.10	0.056	0.043
0.15	0.068	0.051
0.20	0.076	0.057
0.25	0.082	0.060
0.30	0.086	0.062
0.35	0.087	0.063
0.40	0.087	0.062
0.45	0.085	0.059
0.50	0.082	0.055
0.55	0.077	0.051
0.60	0.071	0.045
0.65	0.064	0.039
0.70	0.057	0.033
0.75	0.048	0.026
0.80	0.039	0.020
0.85	0.030	0.015
0.90	0.020	0.010
0.95	0.010	0.005
1.00	0	0

Table I

Lift and Pitching Moment Results

Free Transition					
R = 3 x 10^5			R = 8 x 10^5		
α^o	C_L	C_m	α^o	C_L	C_m
-2.09	0.029	-0.035	-2.04	0.019	-0.033
-0.64	0.143	-0.032	-0.65	0.145	-0.029
0.74	0.269	-0.033	0.69	0.280	-0.035
2.07	0.405	-0.039	2.04	0.408	-0.031
3.40	0.537	-0.032	3.49	0.518	-0.026
4.74	0.665	-0.028	4.88	0.638	-0.018
6.10	0.789	-0.037	6.46	0.739	-0.022
7.77	0.853	-0.023	7.85	0.836	-0.018
9.32	0.936	-0.031	9.35	0.931	-0.019
11.05	0.990	-0.007	11.15	0.969	-0.003
12.78	1.040	-0.004	12.73	1.048	-0.017
0.028" Diameter Transition Wires at 27.5% Chord on Upper and Lower Surfaces					
R = 3 x 10^5			R = 8 x 10^5		
α^o	C_L	C_m	α^o	C_L	C_m
-2.10	0.032	-0.040	-2.01	0.013	-0.034
-0.69	0.153	-0.037	-0.59	0.132	-0.033
0.68	0.280	-0.037	0.76	0.265	-0.029
2.07	0.401	-0.035	2.13	0.381	-0.029
3.47	0.522	-0.028	3.55	0.509	-0.026
4.90	0.634	-0.028	-	-	-
6.25	0.759	-0.033	6.37	0.738	-0.022
7.76	0.854	-0.021	-	-	-
9.33	0.936	-0.020	9.42	0.918	-0.009
11.24	0.953	-0.009	11.08	0.984	-0.010
13.14	0.973	-0.012	-	-	-

0.015" Diameter Transition Wires at 8% Chord on Upper and Lower Surfaces					
$R = 3 \times 10^5$			$R \doteq 8 \times 10^5$		
α^o	C_L	C_m	α^o	C_L	C_m
-2.04	0.019	-0.038	-2.08	-0.008	-0.034
0.72	0.273	-0.031	0.76	0.263	-0.038
3.61	0.496	-0.027	3.66	0.486	-0.029
6.61	0.693	-0.025	6.62	0.678	-0.016
9.50	0.904	-0.016	9.56	0.892	-0.004
11.13	0.973	-0.020	11.28	0.947	-0.007
0.015" Diameter Transition Wires at 4% Chord on Upper and Lower Surfaces					
$R = 3 \times 10^5$			$R \doteq 8 \times 10^5$		
α^o	C_L	C_m	α^o	C_L	C_m
-2.18	0.047	-0.047	-2.00	-0.010	-0.037
0.72	0.273	-0.041	0.73	0.271	-0.025
3.63	0.493	-0.032	3.58	0.502	-0.023
6.58	0.696	-0.025	6.61	0.692	-0.017
9.62	0.873	-0.014	9.80	0.896	-0.006
11.37	0.930	-0.021	11.45	0.914	-0.007
0.015" Diameter Transition Wires at 1% Chord on Upper and Lower Surfaces					
$R = 3 \times 10^5$			$R \doteq 8 \times 10^5$		
α^o	C_L	C_m	α^o	C_L	C_m
-2.21	0.054	-0.036	-2.08	0.027	-0.032
0.59	0.300	-0.037	0.77	0.264	-0.037
3.57	0.504	-0.035	3.73	0.470	-0.027
6.80	0.653	-0.033	6.74	0.666	-0.015
9.65	0.875	-0.017	9.82	0.843	-0.009
11.49	0.905	-0.018	11.55	0.895	-0.002

Table II (concluded)

PRESSURE COEFFICIENT DISTRIBUTIONS

$R = 3 \times 10^5$

Transition Free

	x/c \ α°	-2.09	-0.64	0.74	2.07	3.40	4.74	6.10	7.77	9.32	11.05	12.78
	Leading edge	0.82	1.00	1.02	0.98	0.77	0.33	-0.25	-1.00	-1.78	-2.78	-3.70
Upper Surface	0.025	0.32	0.08	-0.21	-0.53	-0.87	-1.25	-1.64	-2.03	-2.35	-2.72	-3.20
	0.050	0.02	-0.16	-0.40	-0.65	-0.88	-1.17	-1.43	-1.70	-1.95	-2.57	-3.00
	0.075	-0.10	-0.28	-0.49	-0.70	-0.90	-1.13	-1.37	-1.58	-1.76	-2.00	-1.90
	0.10	-0.20	-0.36	-0.55	-0.71	-0.89	-1.08	-1.29	-1.47	-1.63	-1.60	-1.75
	0.15	-0.30	-0.43	-0.58	-0.72	-0.87	-1.00	-1.17	-1.30	-1.38	-1.45	-1.50
	0.20	-0.39	-0.49	-0.63	-0.76	-0.87	-0.98	-1.10	-1.22	-1.20	-1.34	-1.35
	0.25	-0.43	-0.51	-0.64	-0.75	-0.83	-0.93	-1.04	-1.14	-1.10	-1.20	-1.20
	0.30	-0.46	-0.53	-0.64	-0.73	-0.80	-0.88	-0.99	-1.02	-1.03	-1.09	-1.05
	0.35	-0.46	-0.53	-0.63	-0.70	-0.76	-0.83	-0.92	-0.90	-0.92	-0.97	-0.90
	0.40	-0.46	-0.51	-0.60	-0.68	-0.72	-0.78	-0.88	-0.84	-0.84	-0.87	-0.75
	0.45	-0.46	-0.49	-0.57	-0.62	-0.68	-0.74	-0.80	-0.78	-0.77	-0.78	-0.60
	0.50	-0.41	-0.45	-0.52	-0.57	-0.63	-0.70	-0.69	-0.70	-0.68	-0.67	-0.45
	0.55	-0.36	-0.40	-0.48	-0.54	-0.60	-0.66	-0.57	-0.59	-0.55	-0.51	-0.25
	0.60	-0.35	-0.39	-0.48	-0.53	-0.58	-0.41	-0.44	-0.45	-0.42	-0.38	-0.20
	0.65	-0.32	-0.38	-0.45	-0.32	-0.23	-0.28	-0.32	-0.32	-0.28	-0.24	-0.19
	0.70	-0.20	-0.14	-0.11	-0.15	-0.19	-0.22	-0.26	-0.24	-0.20	-0.16	-0.20
	0.75	0.00	-0.01	-0.07	-0.09	-0.11	-0.15	-0.17	-0.16	-0.10	-0.09	-0.20
	0.80	0.01	0.01	-0.03	-0.05	-0.06	-0.08	-0.10	-0.08	-0.05	-0.05	-0.20
Lower Surface	0.025	-0.35	-0.06	0.18	0.40	0.60	0.73	0.85	0.96	1.00	1.05	1.07
	0.050	-0.40	-0.19	0.00	0.17	0.36	0.50	0.62	0.76	0.83	0.93	1.00
	0.075	-0.42	-0.25	-0.10	0.07	0.22	0.35	0.48	0.60	0.69	0.80	0.87
	0.10	-0.45	-0.29	-0.17	-0.02	0.13	0.25	0.37	0.49	0.57	0.69	0.76
	0.15	-0.45	-0.32	-0.22	-0.12	0.00	0.10	0.22	0.32	0.41	0.50	0.57
	0.20	-0.41	-0.30	-0.24	-0.17	-0.07	0.02	0.12	0.20	0.29	0.36	0.43
	0.25	-0.39	-0.29	-0.25	-0.18	-0.08	-0.00	0.10	0.16	0.23	0.31	0.36
	0.30	-0.39	-0.30	-0.28	-0.20	-0.12	-0.06	0.02	0.10	0.16	0.22	0.27
	0.40	-0.30	-0.26	-0.24	-0.19	-0.12	-0.08	0.00	0.03	0.10	0.14	0.18
	0.50	-0.22	-0.17	-0.15	-0.10	-0.06	0.00	0.03	0.07	0.12	0.14	0.17
	0.60	-0.08	-0.09	-0.09	-0.05	-0.00	0.02	0.08	0.10	0.12	0.13	0.14
	0.70	-0.01	0.00	-0.01	0.00	0.02	0.06	0.10	0.11	0.12	0.11	0.11
	0.80	0.02	0.05	0.03	0.03	0.06	0.10	0.11	0.11	0.12	0.10	0.07

Table III (i)

PRESSURE COEFFICIENT DISTRIBUTIONS

$R = 3 \times 10^5$

Transition Wires at 27½% Chord

	x/c \ α°	-2.10	-0.69	0.68	2.07	3.47	4.90	6.25	7.76	9.33	11.24	13.14
	Leading edge	0.80	0.98	1.02	0.96	0.77	0.37	-0.18	-0.91	-1.77	-2.62	-3.40
Upper Surface	0.025	0.31	0.06	-0.22	-0.51	-0.82	-1.21	-1.57	-1.98	-2.37	-2.58	-2.95
	0.050	0.03	-0.18	-0.39	-0.62	-0.86	-1.11	-1.37	-1.66	-1.92	-2.43	-2.92
	0.075	-0.12	-0.30	-0.49	-0.68	-0.89	-1.10	-1.30	-1.54	-1.78	-2.02	-1.77
	0.10	-0.22	-0.38	-0.53	-0.69	-0.89	-1.06	-1.25	-1.45	-1.62	-1.52	-1.58
	0.15	-0.32	-0.46	-0.58	-0.70	-0.85	-0.98	-1.12	-1.28	-1.38	-1.38	-1.38
	0.20	-0.40	-0.52	-0.62	-0.72	-0.84	-0.94	-1.05	-1.18	-1.18	-1.27	-1.22
	0.25	-0.39	-0.49	-0.58	-0.67	-0.77	-0.85	-0.98	-1.08	-1.04	-1.09	-1.02
	0.30	-0.74	-0.83	-0.89	-0.97	-1.03	-1.10	-1.26	-1.01	-1.10	-1.09	-0.95
	0.35	-0.37	-0.44	-0.51	-0.61	-0.77	-0.77	-0.77	-0.87	-0.92	-0.91	-0.77
	0.40	-0.44	-0.49	-0.54	-0.59	-0.63	-0.68	-0.77	-0.83	-0.86	-0.82	-0.62
	0.45	-0.47	-0.53	-0.55	-0.60	-0.64	-0.68	-0.72	-0.78	-0.78	-0.71	-0.45
	0.50	-0.46	-0.49	-0.52	-0.57	-0.59	-0.64	-0.68	-0.69	-0.68	-0.58	-0.31
	0.55	-0.38	-0.42	-0.44	-0.48	-0.49	-0.53	-0.56	-0.58	-0.56	-0.42	-0.24
	0.60	-0.31	-0.34	-0.36	-0.37	-0.39	-0.41	-0.43	-0.44	-0.43	-0.31	-0.24
	0.65	-0.23	-0.24	-0.26	-0.27	-0.28	-0.29	-0.32	-0.32	-0.28	-0.21	-0.23
	0.70	-0.17	-0.19	-0.19	-0.21	-0.22	-0.23	-0.24	-0.24	-0.21	-0.16	-0.25
	0.75	-0.10	-0.12	-0.13	-0.13	-0.14	-0.14	-0.14	-0.15	-0.13	-0.13	-0.26
	0.80	-0.06	-0.07	-0.07	-0.08	-0.08	-0.08	-0.09	-0.09	-0.08	-0.12	-0.27
Lower Surface	0.025	-0.37	-0.09	0.16	0.37	0.57	0.73	0.85	0.93	0.98	1.02	1.03
	0.050	-0.43	-0.22	-0.02	0.16	0.33	0.48	0.63	0.75	0.83	0.91	0.96
	0.075	-0.47	-0.27	-0.10	0.07	0.21	0.34	0.48	0.59	0.68	0.77	0.82
	0.10	-0.48	-0.32	-0.17	-0.02	0.12	0.22	0.37	0.47	0.57	0.63	0.73
	0.15	-0.47	-0.35	-0.22	-0.10	0.02	0.10	0.22	0.31	0.40	0.48	0.53
	0.20	-0.42	-0.33	-0.22	-0.13	-0.03	0.03	0.13	0.21	0.29	0.35	0.40
	0.25	-0.36	-0.27	-0.18	-0.09	-0.02	0.06	0.13	0.20	0.28	0.33	0.38
	0.30	-0.60	-0.54	-0.46	-0.38	-0.32	-0.24	-0.16	-0.08	0.00	0.03	0.09
	0.40	-0.28	-0.24	-0.19	-0.15	-0.08	-0.04	0.00	0.06	0.12	0.13	0.16
	0.50	-0.18	-0.15	-0.12	-0.07	-0.03	0.00	0.03	0.09	0.12	0.12	0.15
	0.60	-0.10	-0.08	-0.05	-0.03	0.01	0.02	0.07	0.10	0.13	0.11	0.13
	0.70	-0.04	-0.04	-0.02	0.01	0.02	0.05	0.08	0.10	0.11	0.09	0.09
	0.80	0.02	0.03	0.03	0.04	0.06	0.08	0.09	0.10	0.10	0.08	0.04

Table III (ii)

PRESSURE COEFFICIENT DISTRIBUTIONS

$R = 3 \times 10^5$

Transition Wires at 8% Chord

	x/c \ c°	-2.04	0.72	3.61	6.61	9.50	11.13
	Leading edge	0.79	1.01	0.75	-0.13	-1.65	-2.60
Upper Surface	0.025	0.30	-0.19	-0.82	-1.50	-2.36	-2.65
	0.050	0.02	-0.36	-0.82	-1.30	-1.86	-2.40
	0.075	-0.08	-0.42	-0.80	-1.19	-1.69	-1.85
	0.10	-0.42	-0.77	-1.12	-1.38	-1.78	-1.64
	0.15	-0.28	-0.52	-0.76	-0.99	-1.19	-1.40
	0.20	-0.40	-0.60	-0.82	-0.98	-1.18	-1.28
	0.25	-0.45	-0.61	-0.79	-0.93	-1.09	-1.17
	0.30	-0.48	-0.62	-0.78	-0.88	-1.00	-1.06
	0.35	-0.49	-0.60	-0.73	-0.82	-0.90	-0.94
	0.40	-0.49	-0.58	-0.69	-0.76	-0.83	-0.87
	0.45	-0.48	-0.57	-0.66	-0.70	-0.76	-0.77
	0.50	-0.47	-0.53	-0.60	-0.62	-0.68	-0.66
	0.55	-0.40	-0.44	-0.50	-0.51	-0.53	-0.50
	0.60	-0.32	-0.35	-0.39	-0.40	-0.40	-0.38
	0.65	-0.22	-0.24	-0.28	-0.28	-0.28	-0.26
	0.70	-0.17	-0.18	-0.22	-0.20	-0.20	-0.18
	0.75	-0.10	-0.11	-0.15	-0.14	-0.14	-0.12
	0.80	-0.07	-0.07	-0.08	-0.08	-0.08	-0.09
Lower Surface	0.025	-0.38	0.17	0.55	0.83	0.98	1.00
	0.050	-0.44	0.00	0.33	0.61	0.81	0.90
	0.075	-0.40	-0.06	0.22	0.49	0.68	0.77
	0.10	-0.69	-0.35	-0.06	0.24	0.50	0.61
	0.15	-0.45	-0.20	0.00	0.22	0.47	0.45
	0.20	-0.44	-0.23	-0.07	0.12	0.25	0.32
	0.25	-0.40	-0.23	-0.08	0.10	0.22	0.28
	0.30	-0.41	-0.27	-0.13	0.00	0.13	0.20
	0.40	-0.33	-0.22	-0.12	-0.02	0.07	0.12
	0.50	-0.19	-0.12	-0.06	0.02	0.10	0.12
	0.60	-0.10	-0.05	-0.01	0.06	0.10	0.12
	0.70	-0.05	0.00	0.01	0.07	0.10	0.11
	0.80	0.00	0.03	0.03	0.08	0.10	0.10

Table III (iii)

PRESSURE COEFFICIENT DISTRIBUTIONS

$R = 3 \times 10^5$

Transition Wires at 4% Chord

	x/c \ α°	-2.18	0.72	3.63	6.58	9.62	11.37
	Leading edge	0.80	1.03	0.77	-0.10	-1.63	-2.50
Upper Surface	0.025	0.33	-0.18	-0.77	-1.43	-2.16	-2.55
	0.050	-0.21	-0.69	-1.18	-1.65	-2.22	-2.45
	0.075	-0.07	-0.39	-0.76	-1.27	-1.67	-1.70
	0.10	-0.20	-0.50	-0.78	-1.06	-1.36	-1.48
	0.15	-0.30	-0.57	-0.80	-1.02	-1.29	-1.38
	0.20	-0.41	-0.62	-0.83	-1.00	-1.20	-1.27
	0.25	-0.46	-0.63	-0.80	-0.94	-1.10	-1.12
	0.30	-0.49	-0.65	-0.77	-0.88	-1.00	-1.02
	0.35	-0.49	-0.62	-0.73	-0.82	-0.90	-0.88
	0.40	-0.49	-0.60	-0.68	-0.76	-0.83	-0.78
	0.45	-0.48	-0.58	-0.65	-0.70	-0.75	-0.68
	0.50	-0.44	-0.55	-0.59	-0.64	-0.64	-0.55
	0.55	-0.39	-0.49	-0.49	-0.52	-0.50	-0.40
	0.60	-0.37	-0.38	-0.38	-0.40	-0.37	-0.28
	0.65	-0.35	-0.26	-0.27	-0.28	-0.25	-0.19
	0.70	-0.19	-0.19	-0.20	-0.20	-0.17	-0.18
	0.75	-0.05	-0.13	-0.13	-0.13	-0.11	-0.17
	0.80	-0.03	-0.07	-0.07	-0.07	-0.08	-0.16
Lower Surface	0.025	-0.32	0.18	0.58	0.83	1.00	1.00
	0.050	-0.70	-0.28	0.13	0.48	0.84	0.90
	0.075	-0.48	-0.08	0.23	0.48	0.69	0.73
	0.10	-0.40	-0.18	0.12	0.36	0.55	0.62
	0.15	-0.45	-0.25	0	0.20	0.39	0.45
	0.20	-0.42	-0.26	-0.06	0.10	0.27	0.33
	0.25	-0.39	-0.25	-0.08	0.07	0.22	0.28
	0.30	-0.39	-0.27	-0.10	0.01	0.13	0.20
	0.40	-0.31	-0.24	-0.10	-0.02	0.08	0.12
	0.50	-0.17	-0.15	-0.04	0.02	0.10	0.12
	0.60	-0.10	-0.08	0	0.05	0.10	0.10
	0.70	-0.03	0	0.02	0.07	0.10	0.07
	0.80	0.02	0.03	0.05	0.09	0.10	0.05

Table III (iv)

PRESSURE COEFFICIENT DISTRIBUTIONS

$R = 3 \times 10^5$

Transition Wires at 1% Chord

	x/c \ α°	-2.21	0.59	3.57	6.80	9.65	11.49
	Leading edge	0.82	1.00	0.80	-0.05	-1.50	-2.44
Upper Surface	0.025	0.30	-0.18	-0.98	-1.87	-2.87	-3.24
	0.050	0.02	-0.38	-0.77	-1.08	-1.52	-1.71
	0.075	-0.13	-0.48	-0.83	-1.16	-1.57	-1.69
	0.10	-0.23	-0.53	-0.84	-1.10	-1.45	-1.55
	0.15	-0.32	-0.58	-0.82	-1.03	-1.30	-1.35
	0.20	-0.42	-0.63	-0.83	-0.99	-1.20	-1.23
	0.25	-0.47	-0.64	-0.80	-0.93	-1.10	-1.10
	0.30	-0.48	-0.65	-0.78	-0.87	-1.01	-0.97
	0.35	-0.49	-0.62	-0.74	-0.80	-0.90	-0.83
	0.40	-0.49	-0.59	-0.69	-0.74	-0.82	-0.71
	0.45	-0.49	-0.57	-0.67	-0.68	-0.73	-0.56
	0.50	-0.45	-0.53	-0.60	-0.61	-0.60	-0.41
	0.55	-0.39	-0.48	-0.51	-0.50	-0.47	-0.28
	0.60	-0.38	-0.47	-0.40	-0.38	-0.36	-0.24
	0.65	-0.35	-0.40	-0.28	-0.27	-0.24	-0.22
	0.70	-0.20	-0.12	-0.21	-0.20	-0.17	-0.23
	0.75	-0.05	-0.08	-0.14	-0.14	-0.13	-0.23
	0.80	-0.03	-0.05	-0.08	-0.07	-0.11	-0.23
Lower Surface	0.025	-0.60	0.22	0.58	0.81	0.99	1.02
	0.050	-0.35	0.00	0.33	0.60	0.82	0.87
	0.075	-0.42	-0.08	0.22	0.45	0.67	0.73
	0.10	-0.44	-0.16	0.13	0.35	0.54	0.62
	0.15	-0.46	-0.22	0.00	0.20	0.38	0.55
	0.20	-0.43	-0.22	-0.07	0.10	0.26	0.32
	0.25	-0.39	-0.22	-0.08	0.07	0.22	0.27
	0.30	-0.39	-0.25	-0.11	0.01	0.13	0.18
	0.40	-0.31	-0.21	-0.11	-0.02	0.07	0.11
	0.50	-0.18	-0.13	-0.05	0.02	0.09	0.11
	0.60	-0.10	-0.07	0.00	0.05	0.10	0.09
	0.70	-0.03	0.00	0.03	0.07	0.08	0.07
	0.80	0.02	0.06	0.07	0.08	0.07	0.04

Table III (v)

PRESSURE DISTRIBUTIONS

R ≙ 8 x 10^5

Transition Free

	x/c \ α°	-2.04	-0.55	0.69	2.04	3.49	4.88	6.46	7.85	9.35	11.15	12.73
	Leading edge	0.80	1.00	1.00	0.98	0.75	0.34	0.24	-0.98	-1.91	-2.88	-3.88
Upper Surface	0.025	0.32	0.07	-0.21	-0.52	-0.86	-1.23	-1.60	-2.01	-2.45	-2.88	-3.32
	0.05	0.05	-0.17	-0.39	-0.62	-0.87	-1.13	-1.40	-1.68	-2.02	-2.08	-2.24
	0.075	-0.10	-0.29	-0.48	-0.69	-0.89	-1.12	-1.34	-1.57	-1.75	-1.88	-2.02
	0.10	-0.19	-0.36	-0.53	-0.71	-0.88	-1.07	-1.26	-1.44	-1.45	-1.65	-1.74
	0.15	-0.30	-0.44	-0.58	-0.72	-0.86	-1.00	-1.15	-1.21	-1.34	-1.46	-1.50
	0.20	-0.40	-0.51	-0.63	-0.75	-0.86	-0.97	-1.07	-1.14	-1.26	-1.34	-1.34
	0.25	-0.44	-0.54	-0.64	-0.74	-0.83	-0.93	-0.99	-1.06	-1.16	-1.21	-1.18
	0.30	-0.46	-0.55	-0.63	-0.72	-0.79	-0.88	-0.91	-0.98	-1.05	-1.08	-1.02
	0.35	-0.47	-0.55	-0.62	-0.70	-0.76	-0.83	-0.84	-0.89	-0.95	-0.97	-0.88
	0.40	-0.47	-0.53	-0.60	-0.67	-0.72	-0.75	-0.78	-0.83	-0.87	-0.86	-0.76
	0.45	-0.47	-0.53	-0.59	-0.64	-0.70	-0.68	-0.73	-0.77	-0.79	-0.77	-0.63
	0.50	-0.45	-0.50	-0.55	-0.61	-0.65	-0.63	-0.66	-0.69	-0.70	-0.65	-0.48
	0.55	-0.39	-0.44	-0.50	-0.55	-0.51	-0.52	-0.54	-0.56	-0.56	-0.49	-0.33
	0.60	-0.36	-0.39	-0.36	-0.33	-0.35	-0.39	-0.41	-0.43	-0.42	-0.34	-0.30
	0.65	-0.15	-0.18	-0.21	-0.24	-0.27	-0.29	-0.30	-0.31	-0.30	-0.21	-0.27
	0.70	-0.12	-0.14	-0.17	-0.19	-0.21	-0.21	-0.22	-0.22	-0.20	-0.13	-0.27
	0.75	-0.05	-0.07	-0.08	-0.10	-0.11	-0.12	-0.13	-0.13	-0.11	-0.09	-0.25
	0.80	0.00	-0.01	-0.03	-0.03	-0.05	-0.05	-0.05	-0.05	-0.04	-0.06	-0.24
Lower Surface	0.025	-0.38	-0.08	0.17	0.39	0.58	0.73	0.86	0.95	1.01	1.04	1.04
	0.05	-0.44	-0.21	-0.01	0.18	0.35	0.50	0.63	0.74	0.84	0.91	0.96
	0.075	-0.45	-0.26	-0.09	0.07	0.23	0.36	0.49	0.60	0.70	0.79	0.85
	0.10	-0.47	-0.31	-0.16	-0.01	0.12	0.25	0.37	0.48	0.58	0.66	0.73
	0.15	-0.47	-0.35	-0.23	-0.11	0.01	0.11	0.22	0.32	0.41	0.49	0.55
	0.20	-0.43	-0.34	-0.24	-0.15	-0.06	0.03	0.13	0.21	0.28	0.35	0.41
	0.25	-0.40	-0.31	-0.23	-0.15	-0.07	0.01	0.09	0.17	0.23	0.30	0.35
	0.30	-0.39	-0.32	-0.25	-0.17	-0.10	-0.03	0.04	0.11	0.17	0.23	0.27
	0.40	-0.34	-0.28	-0.23	-0.17	-0.12	-0.06	-0.01	0.05	0.09	0.14	0.17
	0.50	-0.17	-0.17	-0.14	-0.03	-0.05	-0.01	0.04	0.08	0.11	0.14	0.15
	0.60	-0.08	-0.06	-0.03	0.01	0.01	0.03	0.06	0.09	0.11	0.13	0.14
	0.70	-0.04	-0.02	0.00	0.02	0.04	0.05	0.07	0.10	0.11	0.11	0.10
	0.80	0.03	0.03	0.05	0.06	0.07	0.08	0.09	0.10	0.10	0.09	0.07

Table IV (i)

PRESSURE COEFFICIENT DISTRIBUTIONS

$R \simeq 8 \times 10^5$

Transition Wires at 27½% Chord.

	x/c \ α°	-2.01	-0.59	0.76	2.13	3.55	6.37	9.42	11.08
	Leading edge	0.79	0.99	1.02	0.98	0.76	-0.22	-1.84	-2.78
Upper Surface	0.025	0.33	0.07	-0.20	-0.51	-0.84	-1.60	-2.40	-2.81
	0.050	0.05	-0.16	-0.38	-0.61	-0.89	-1.38	-2.00	-2.05
	0.075	-0.10	-0.28	-0.47	-0.68	-0.89	-1.33	-1.72	-1.84
	0.10	-0.19	-0.35	-0.52	-0.69	-0.87	-1.24	-1.43	-1.61
	0.15	-0.30	-0.43	-0.56	-0.71	-0.84	-1.13	-1.31	-1.42
	0.20	-0.38	-0.50	-0.60	-0.72	-0.83	-1.04	-1.21	-1.29
	0.25	-0.38	-0.48	-0.57	-0.66	-0.77	-0.89	-1.04	-1.11
	0.30	-0.70	-0.80	-0.89	-0.98	-1.07	-1.08	-1.23	-1.26
	0.35	-0.41	-0.48	-0.54	-0.60	-0.70	-0.82	-0.93	-0.95
	0.40	-0.44	-0.50	-0.56	-0.61	-0.70	-0.77	-0.85	-0.86
	0.45	-0.44	-0.50	-0.55	-0.59	-0.64	-0.72	-0.77	-0.77
	0.50	-0.43	-0.48	-0.52	-0.55	-0.59	-0.65	-0.68	-0.65
	0.55	-0.36	-0.39	-0.43	-0.45	-0.49	-0.53	-0.54	-0.50
	0.60	-0.27	-0.30	-0.32	-0.35	-0.37	-0.40	-0.41	-0.37
	0.65	-0.19	-0.22	-0.24	-0.25	-0.27	-0.30	-0.29	-0.25
	0.70	-0.14	-0.16	-0.17	-0.19	-0.20	-0.21	-0.20	-0.16
	0.75	-0.07	-0.08	-0.09	-0.10	-0.11	-0.12	-0.11	-0.10
	0.80	-0.02	-0.02	-0.03	-0.04	-0.04	-0.05	-0.04	-0.05
Lower Surface	0.025	-0.38	-0.09	0.17	0.39	0.57	0.85	1.00	1.03
	0.050	-0.44	-0.22	-0.11	0.18	0.34	0.63	0.83	0.90
	0.075	-0.45	-0.26	-0.09	0.08	0.22	0.49	0.69	0.78
	0.10	-0.47	-0.31	-0.16	-0.01	0.12	0.37	0.57	0.65
	0.15	-0.46	-0.34	-0.22	-0.10	0.01	0.22	0.40	0.48
	0.20	-0.42	-0.32	-0.23	-0.14	-0.04	0.13	0.29	0.36
	0.25	-0.34	-0.26	-0.17	-0.09	-0.01	0.14	0.28	0.34
	0.30	-0.43	-0.36	-0.29	-0.21	-0.14	0.00	0.13	0.20
	0.40	-0.30	-0.26	-0.21	-0.16	-0.11	0.00	0.10	0.15
	0.50	-0.19	-0.15	-0.12	-0.08	-0.04	0.04	0.11	0.14
	0.60	-0.10	-0.07	-0.05	-0.02	0.01	0.06	0.11	0.13
	0.70	-0.05	-0.03	-0.01	0.01	0.03	0.07	0.10	0.11
	0.80	0.01	0.02	0.03	0.05	0.06	0.08	0.10	0.09

Table IV (ii)

PRESSURE COEFFICIENT DISTRIBUTIONS

$R \triangleq 8 \times 10^5$

Transition Wires at 8% Chord.

	x/c \ α°	-2.08	0.76	3.66	6.62	9.56	11.28
	Leading edge	0.78	1.03	0.77	-0.16	-1.74	-2.63
Upper Surface	0.025	0.33	-0.19	-0.82	-1.56	-2.37	-2.69
	0.050	0.05	-0.35	-0.82	-1.34	-1.94	-1.94
	0.075	-0.06	-0.42	-0.81	-1.26	-1.56	-1.68
	0.10	-0.30	-0.66	-1.01	-1.36	-1.71	-1.86
	0.15	-0.28	-0.53	-0.79	-1.03	-1.31	-1.39
	0.20	-0.38	-0.61	-0.82	-1.02	-1.22	-1.27
	0.25	-0.43	-0.62	-0.79	-0.96	-1.12	-1.14
	0.30	-0.45	-0.62	-0.76	-0.89	-1.01	-1.03
	0.35	-0.45	-0.59	-0.71	-0.82	-0.92	-0.90
	0.40	-0.46	-0.58	-0.68	-0.77	-0.84	-0.81
	0.45	-0.46	-0.55	-0.64	-0.71	-0.75	-0.71
	0.50	-0.44	-0.52	-0.59	-0.63	-0.65	-0.59
	0.55	-0.36	-0.43	-0.48	-0.51	-0.51	-0.43
	0.60	-0.27	-0.32	-0.36	-0.38	-0.37	-0.30
	0.65	-0.20	-0.24	-0.27	-0.28	-0.25	-0.20
	0.70	-0.14	-0.18	-0.20	-0.19	-0.16	-0.15
	0.75	-0.07	-0.09	-0.11	-0.10	-0.10	-0.13
	0.80	-0.02	-0.03	-0.04	-0.05	-0.05	-0.10
Lower Surface	0.025	-0.38	0.16	0.57	0.87	1.00	1.01
	0.050	-0.44	-0.01	0.34	0.61	0.82	0.88
	0.075	-0.39	-0.04	0.25	0.50	0.70	0.77
	0.10	-0.84	-0.47	-0.13	0.17	0.45	0.55
	0.15	-0.46	-0.22	0.00	0.25	0.39	0.47
	0.20	-0.46	-0.27	-0.08	0.09	0.26	0.33
	0.25	-0.40	-0.24	-0.08	0.07	0.21	0.28
	0.30	-0.38	-0.24	-0.10	0.03	0.15	0.20
	0.40	-0.32	-0.23	-0.12	-0.01	0.08	0.11
	0.50	-0.19	-0.13	-0.05	0.02	0.09	0.11
	0.60	-0.11	-0.05	-0.01	0.05	0.10	0.11
	0.70	-0.05	-0.02	-0.01	0.05	0.08	0.08
	0.80	-0.01	0.02	0.04	0.06	0.08	0.07

Table IV (iii)

PRESSURE COEFFICIENT DISTRIBUTIONS

R = 8 x 10^5

Transition Wires at 4% Chord

	x/c \ α^c	-2.00	0.73	3.58	6.61	9.80	11.45
	Leading edge	0.79	1.03	0.77	-0.15	-1.72	-2.58
Upper Surface	0.025	0.34	-0.17	-0.78	-1.52	-2.23	-2.63
	0.050	-0.26	-0.79	-1.36	-2.00	-1.61	-1.92
	0.075	-0.05	-0.39	-0.76	-1.16	-1.64	-1.80
	0.10	-0.16	-0.47	-0.78	-1.13	-1.45	-1.57
	0.15	-0.32	-0.54	-0.80	-1.07	-1.30	-1.38
	0.20	-0.38	-0.60	-0.82	-1.04	-1.21	-1.25
	0.25	-0.43	-0.62	-0.79	-0.98	-1.10	-1.11
	0.30	-0.45	-0.61	-0.76	-0.90	-1.00	-0.98
	0.35	-0.45	-0.59	-0.71	-0.83	-0.90	-0.85
	0.40	-0.45	-0.57	-0.67	-0.78	-0.81	-0.73
	0.45	-0.45	-0.56	-0.64	-0.72	-0.71	-0.60
	0.50	-0.44	-0.51	-0.58	-0.63	-0.60	-0.45
	0.55	-0.36	-0.43	-0.48	-0.51	-0.45	-0.30
	0.60	-0.27	-0.33	-0.36	-0.38	-0.31	-0.23
	0.65	-0.20	-0.24	-0.26	-0.27	-0.21	-0.20
	0.70	-0.15	-0.17	-0.19	-0.19	-0.14	-0.20
	0.75	-0.07	-0.09	-0.11	-0.11	-0.09	-0.19
	0.80	-0.02	-0.03	-0.04	-0.04	-0.06	-0.19
Lower Surface	0.025	-0.33	0.18	0.57	0.86	1.00	1.01
	0.050	-0.88	-0.35	0.11	0.46	0.84	0.89
	0.075	-0.34	-0.01	0.26	0.49	0.69	0.75
	0.10	-0.43	-0.14	0.12	0.35	0.55	0.63
	0.15	-0.46	-0.22	0.00	0.20	0.38	0.46
	0.20	-0.45	-0.26	-0.07	0.09	0.26	0.33
	0.25	-0.39	-0.23	-0.07	0.07	0.21	0.27
	0.30	-0.37	-0.24	-0.10	0.02	0.15	0.20
	0.40	-0.31	-0.22	-0.11	-0.02	0.08	0.11
	0.50	-0.19	-0.13	-0.05	0.01	0.09	0.11
	0.60	-0.10	-0.05	0.00	0.05	0.09	0.10
	0.70	-0.05	-0.03	0.01	0.05	0.08	0.08
	0.80	0.01	0.03	0.04	0.05	0.06	0.05

Table IV (iv)

PRESSURE COEFFICIENT DISTRIBUTIONS

$R \doteq 8 \times 10^5$

Transition Wires at 1% Chord

	x/c \ α°	-2.08	0.77	3.73	6.74	9.82	11.55
	Leading edge	0.82	1.03	0.78	-0.08	-1.55	-2.33
Upper Surface	0.025	0.33	-0.14	-0.70	-1.39	-2.31	-2.55
	0.050	0.04	-0.37	-0.81	-1.31	-1.78	-1.95
	0.075	-0.10	-0.46	-0.83	-1.25	-1.64	-1.76
	0.10	-0.19	-0.48	-0.79	-1.14	-1.44	-1.52
	0.15	-0.30	-0.54	-0.80	-1.07	-1.28	-1.32
	0.20	-0.40	-0.60	-0.81	-1.02	-1.18	-1.18
	0.25	-0.43	-0.62	-0.78	-0.96	-1.07	-1.03
	0.30	-0.46	-0.61	-0.75	-0.89	-0.97	-0.89
	0.35	-0.47	-0.59	-0.71	-0.82	-0.86	-0.75
	0.40	-0.46	-0.57	-0.67	-0.76	-0.76	-0.62
	0.45	-0.46	-0.55	-0.63	-0.70	-0.65	-0.46
	0.50	-0.44	-0.52	-0.58	-0.62	-0.53	-0.34
	0.55	-0.36	-0.43	-0.47	-0.50	-0.37	-0.26
	0.60	-0.27	-0.33	-0.35	-0.38	-0.25	-0.24
	0.65	-0.20	-0.24	-0.26	-0.27	-0.17	-0.24
	0.70	-0.15	-0.17	-0.19	-0.18	-0.15	-0.25
	0.75	-0.07	-0.09	-0.10	-0.10	-0.14	-0.25
	0.80	-0.02	-0.04	-0.04	-0.04	-0.12	-0.24
Lower Surface	0.025	-0.17	0.27	0.56	0.84	0.99	1.02
	0.050	-0.40	-0.01	0.33	0.61	0.81	0.88
	0.075	-0.42	-0.08	0.21	0.47	0.67	0.75
	0.10	-0.44	-0.16	0.11	0.35	0.55	0.63
	0.15	-0.45	-0.22	-0.01	0.20	0.37	0.45
	0.20	-0.44	-0.26	-0.01	0.11	0.25	0.32
	0.25	-0.39	-0.22	-0.08	0.07	0.21	0.26
	0.30	-0.37	-0.23	-0.11	0.02	0.14	0.19
	0.40	-0.31	-0.21	-0.12	-0.02	0.07	0.10
	0.50	-0.18	-0.12	-0.05	0.01	0.08	0.10
	0.60	-0.09	-0.05	-0.01	0.05	0.08	0.09
	0.70	-0.04	-0.01	0.03	0.05	0.07	0.06
	0.80	0.02	0.03	0.05	0.05	0.07	0.03

Table IV (v)

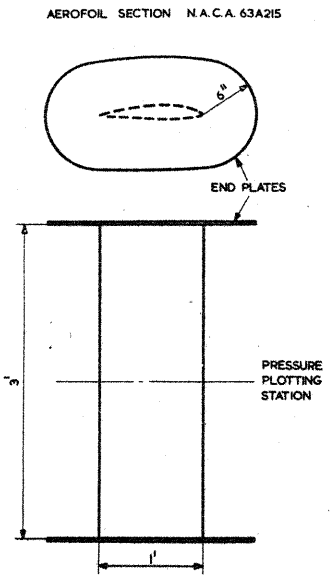

FIG. I. DIAGRAM OF MODEL.

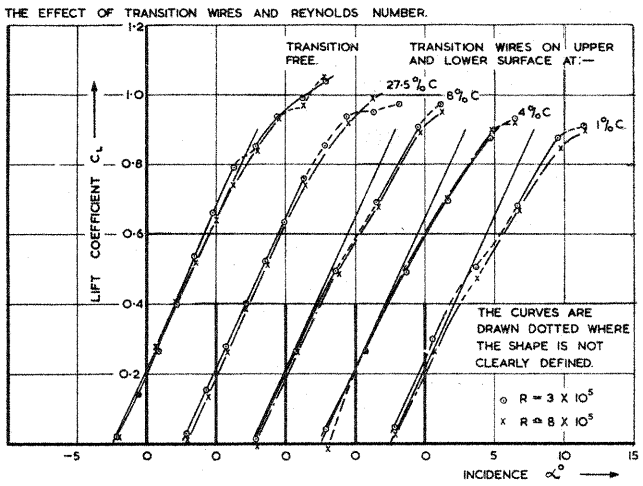

FIG. 2. LIFT CHARACTERISTICS.

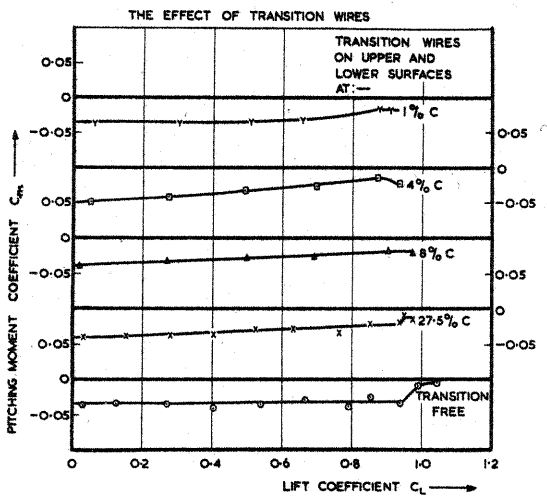

FIG. 3. PITCHING MOMENT CHARACTERISTICS MEASURED AT R = 3 x 10⁵

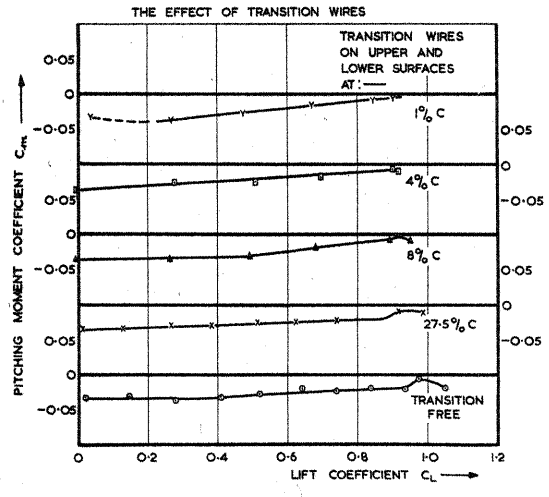

FIG. 4. PITCHING MOMENT CHARACTERISTICS MEASURED AT R ≏ 8 x 10⁵

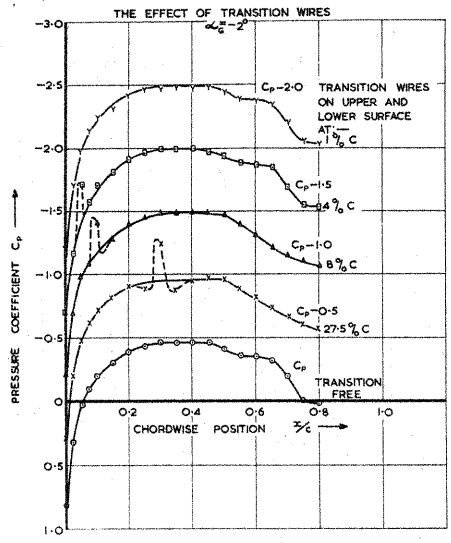

FIG. 5a. MEASURED UPPER SURFACE PRESSURE DISTRIBUTIONS AT $R = 3 \times 10^5$

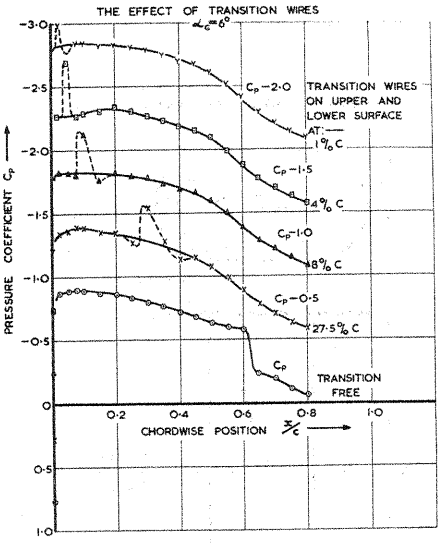

FIG. 5b. MEASURED UPPER SURFACE PRESSURE DISTRIBUTIONS AT $R = 3 \times 10^5$

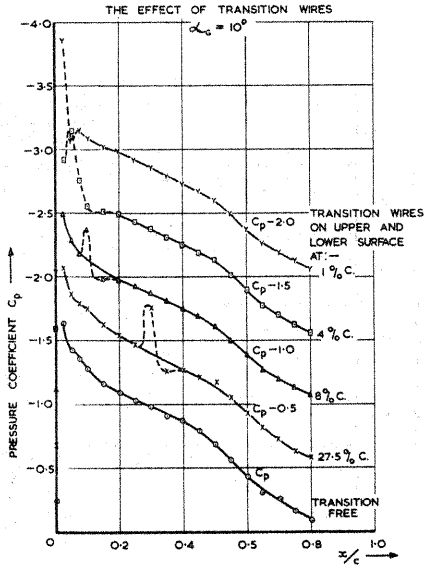

FIG. 5c. MEASURED UPPER SURFACE PRESSURE DISTRIBUTIONS AT $R = 3 \times 10^5$

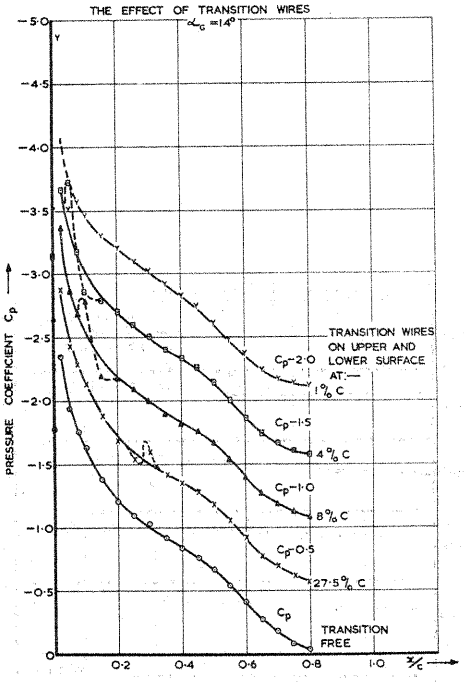

FIG. 5d. MEASURED UPPER SURFACE PRESSURE DISTRIBUTIONS AT $R = 3 \times 10^5$

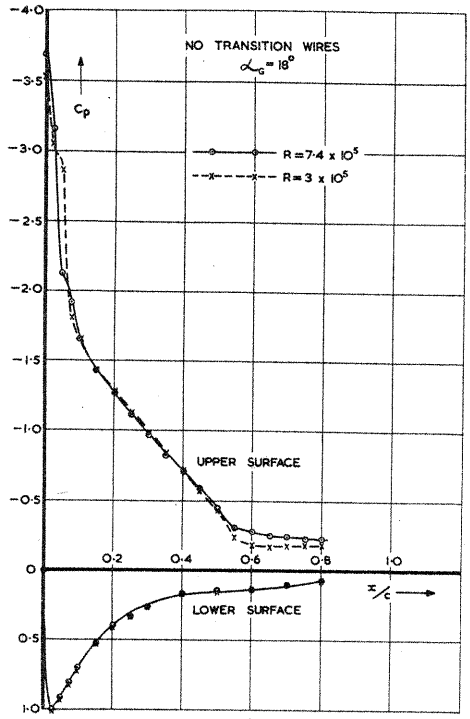

FIG. 6. COMPARISON OF PRESSURE DISTRIBUTIONS NEAR THE STALL AT TWO VALUES OF THE REYNOLDS NUMBER.

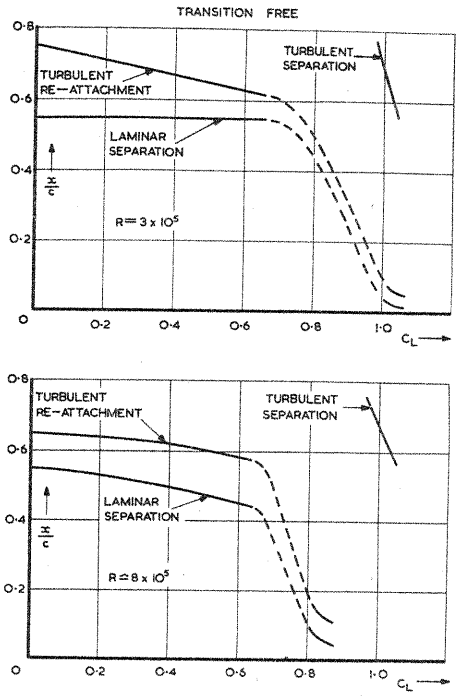

FIG. 7. THE APPROXIMATE CHORDWISE POSITIONS OF LAMINAR SEPARATION. TURBULENT RE-ATTACHMENT AND TURBULENT SEPARATION

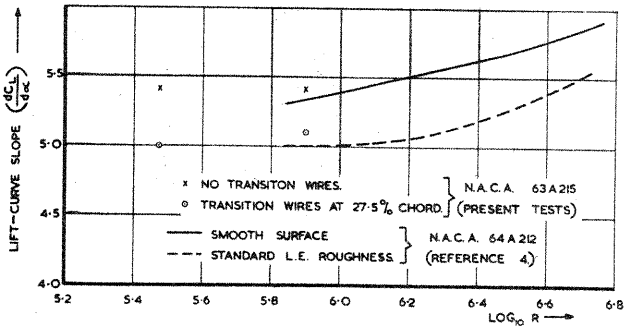

FIG. 8. COMPARISON OF LIFT-CURVE SLOPES FOR TEST SECTION (N.A.C.A. 63A215) WITH N.A.C.A. SECTION 64A212 (REF 4.)